Electronic Supplementary Material (ESI) for Lab on a Chip.

Design and validation of a flowless gradient generating microfluidic device for high-throughput drug testing

Ketaki Bachal[1], Shital Yadav[1], Prasanna Gandhi[2#], Abhijit Majumder[1*]

*[1] Department of Chemical Engineering; Indian Institute of Technology Bombay, Mumbai- 400076, Maharashtra, India. [2] Department of Mechanical Engineering; Indian Institute of Technology Bombay, Mumbai- 400076, Maharashtra, India. #Email: gandhi.iitb@gmail.com *Email: abhijitm@iitb.ac.in*

Abstract

Drug testing is a vital step in identifying the potential efficacy of any new/existing drug and/or combinations of drugs. Conventional methods of testing the efficacy of new drugs using multi-well plates are time-consuming and prone to evaporation loss and manual error. Microfluidic devices with automated generation of concentration gradient provide a promising alternative. The implementation of such microfluidic devices is still limited owing to the additional expertise and facilities required to fabricate and run these devices. Conventional microfluidic devices also need pumps, tubings, valves, and other accessories, making them bulky and nonportable. To address these problems, we have developed a method for fabricating microfluidic structures using a nonconventional technique by exploiting the Saffman-Taylor instability in lifted Hele-Shaw cell. Multi-channel structure molds with varying dimensions were fabricated by shaping ceramic polymer slurry and retaining the shape. Further using the mold thus made, polydimethyl siloxane (PDMS) devices offering static, stable, diffusion-based gradient were casted using soft lithography. We have demonstrated with COMSOL simulation, as well as using Fluorescein isothiocyanate (FITC), a fluorescent dye, that the concentration gradient can be generated in this device, which remains stable for at least 5 days. Using this multichannel device, *in vitro* drug efficacy was validated with two drugs namely- Temozolomide (TMZ) and Curcumin, one FDA approved and one under research, on glioblastoma cells (U87MG). The resulting IC_{50} values were consistent with those reported in literature. We have also demonstrated the possibility of conducting molecular assays post-drug testing in the device by microtubule staining after curcumin treatment on cervical cancer cells (HeLa). In summary, we have demonstrated a i) user-friendly, ii) portable, static drug testing platform that iii) does not require further accessories and can create iv) a stable gradient for long duration. Such a device can reduce the time, manual errors, fabrication and running expenditure, and resources to a great extent in drug testing.

Keywords: High throughput drug testing, diffusion-based gradient, microfluidic device

Supplementary figures-

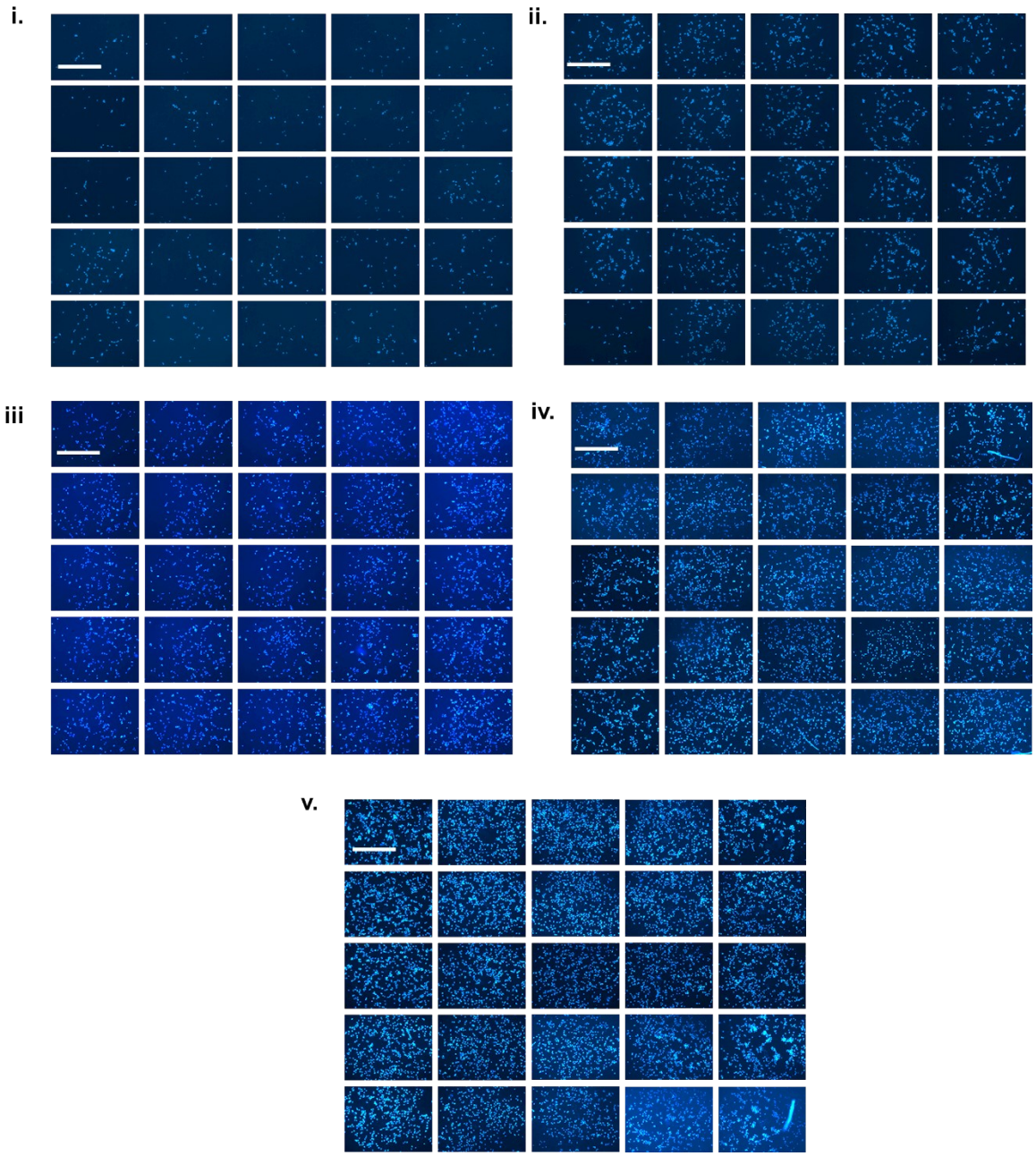

Supplementary figure 1: Equal distribution of cells at the nodes of device represented by Hoechst stained cells at 25 nodes of device with seeding density of- i) 0.25 x 10^5 ii) 0.5 x 10^5, iii) 1.0 x 10^5, iv) 2.0 x 10^5 and v) 4.0 x 10^5 (Scale bar 400 µm).

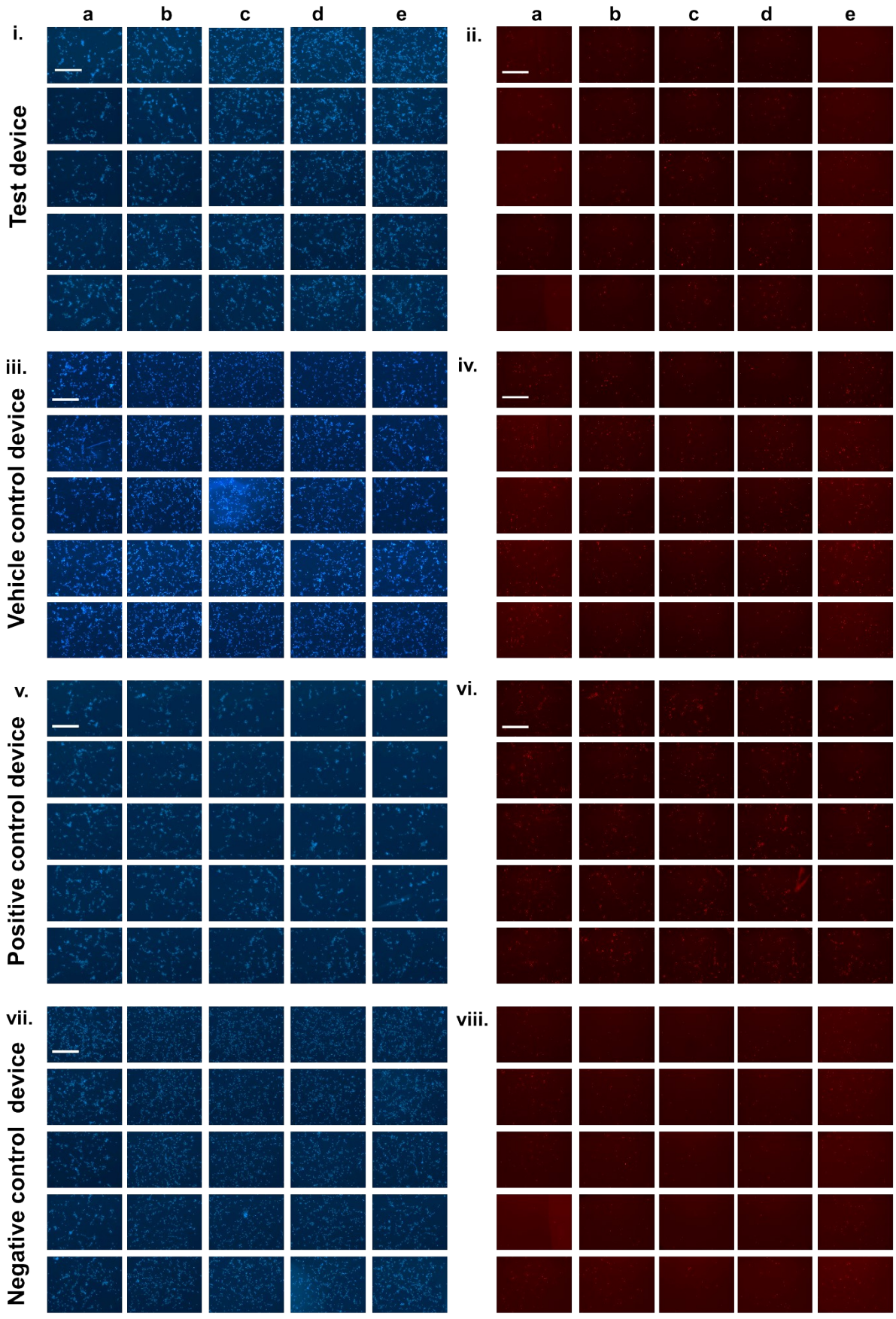
a
b
c
d
e
i.
ii.
Test device
iii.
iv.
Vehicle control device
v.
vi.
Positive control device
vii.
viii.
Negative control device

Supplementary figure 2: Drug testing in device with TMZ. i) Test device with increasing Hoechst stained cells from source to sink (a to e) at 25 nodes ii) Test device with PI stained cells at the corresponding nodes represented in (i), indicating the dead cell population at the 25 nodes of device from source to sink (a-e). iii) DMSO control device with Hoechst staining indicating equal number of cells at all the 25 nodes. iv DMSO control device with PI staining at the corresponding nodes represented in (iii), indicating equal number of dead cells at all the 25 nodes. v) Positive control device with Hoechst stained cells at 25 nodes. vi) Positive control device with PI stained cells at 25 nodes of device. vii) Negative control device with Hoechst stained cells at 25 nodes viii) Negative control device with PI stained cells at the corresponding nodes represented in (vii). (Scale bar 400 µm)

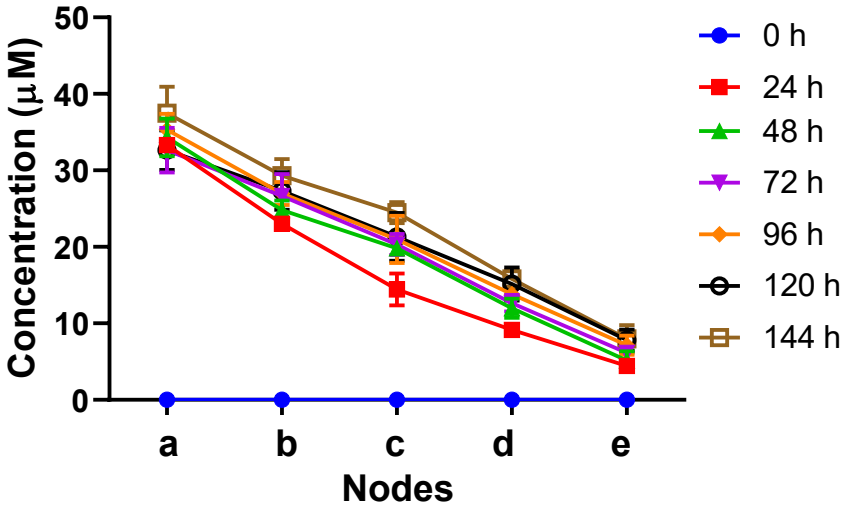

Supplementary figure 3: FITC concentration gradient profile with respect to time (up to 144 h) at different node locations in the microfluidic device.

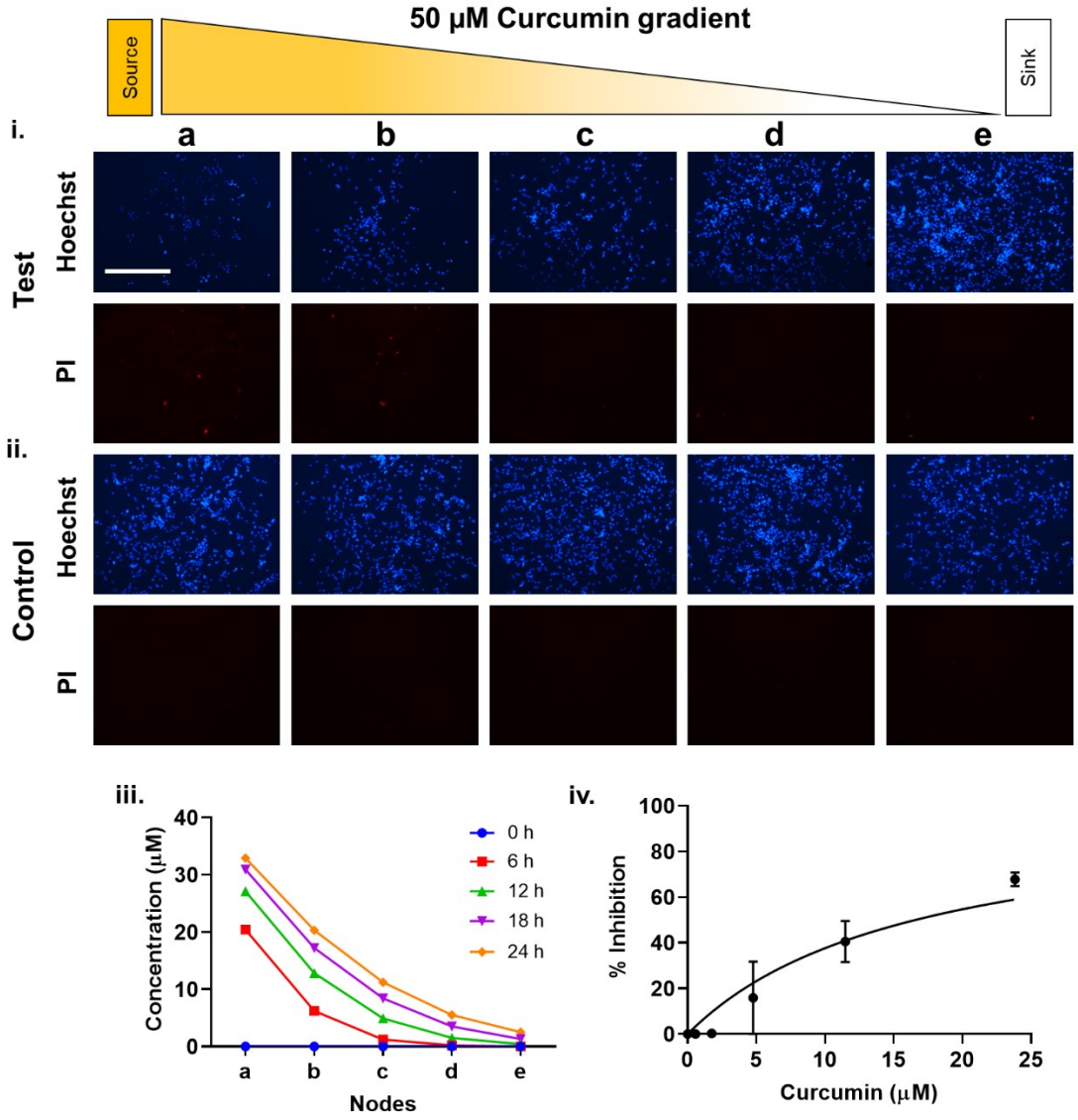

Supplementary figure 4: Estimation of curcumin efficacy using the device: i) Test device: Effect of Curcumin (50 µM) gradient on U87-MG cells was determined using Hoechst and PI staining from source to sink (a-e) in device. ii) Control device: Hoechst and PI staining at 5 nodes (a-e) of the device. iii) Simulation graph of curcumin gradient using COMSOL at 0 h, 6 h, 12 h, 18 h, and 24 h. iv) Percentage inhibition of U87 MG cells at different concentration of curcumin at 5 different nodes from source to sink (a-e) gave IC_{50} as 16.6 µM ± 5.5 µM (Scale bar 400 µm).

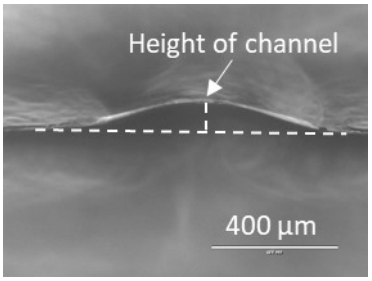

Supplementary figure 5: Cross sectional phase contrast image of the channel.

Sr. No.	Node height (µm)	Channel height (µm)
	N1	N1
1	180.5	78.6
2	177.4	58.5
3	181.6	56.0
4	184.6	84.0
5	191.0	83.0
6	189.6	55.8
7	186.6	60.3
8	187.4	63.8
9	178.4	63.8
10	150.8	46.3
11	169.8	49.9
12	167.9	81.3
13	169.1	55.4
14	155.2	
15	164.9	
16	144.0	
17	174.2	
18	183.3	
19	178.7	
20	187.1	
21	182.5	
22	178.9	
23	174.8	
24	169.6	
25	172.2	
Average	**175.2**	**64.4**
SD	**±12.0**	**±13.0**

Supplementary table 1: The height of node and channels were measured using WLI (White light interferometry) at 25 and 13 positions respectively.

Sr. No.	Node diameter (µm)			Channel width (µm)		
	N1	N2	N3	N1	N2	N3
1	1454.0	1482.7	1461.2	588.9	685.9	677.1
2	1459.9	1488.6	1426.8	531.0	646.0	659.4
3	1420.8	1473.5	1297.1	606.2	672.6	694.8
4	1520.8	1335.3	1270.8	606.3	584.3	593.1
5	1389.2	1278.4	1400.4	628.4	570.8	584.1
6	1430.4	1401.8	1259.3	624.0	592.9	570.9
7	1446.0	1268.9	1290.0	650.5	557.5	579.7
8	1449.0	1314.1	1351.2	708.0	615.0	610.7
9	1453.1	1361.3	1400.8	632.8	619.5	623.9
10	1331.7	1422.8	1354.8	650.5	632.9	650.5
11	1464.4	1314.8	1446.1	628.4	619.5	619.5
12	1439.3	1486.2	1311.1	597.3	655.0	677.0
13	1346.1	1306.1	1415.1	655.0	716.9	721.4
14	1370.8	1417.4	1405.2	637.2	619.5	632.8
15	1398.7	1392.3	1398.2	637.2	659.3	668.4
16	1274.3	1414.2	1371.3	632.7	632.9	646.2
17	1390.9	1367.3	1425.7	716.8	606.2	624.0
18	1295.6	1445.6	1380.1	699.3	650.5	650.7
19	1317.3	1398.7	1464.3	628.7	663.7	668.2
20	1234.0	1423.6	1448.2	650.5	646.1	664.1
21	1399.8	1425.1	1405.2	654.9	654.9	646.6
22	1244.6	1444.5	1362.1	632.8	743.4	721.2
23	1370.7	1379.8	1511.5	659.4	747.8	765.9
24	1289.8	1542.9	1390.3	592.9	650.5	668.2
25	1459.8	1392.5	1468.9	606.3	659.4	650.5
Average	**1386.0**	**1399.1**	**1388.6**	**634.2**	**644.1**	**650.7**
SD	±76.7	±69.8	±65.2	±39.3	±47.0	±46.2

Supplementary table 2: Characterisation of the device. The table indicates the node diameter at 25 nodes of 3 individual devices and channel width of 3 devices measured adjacent to the 25 nodes as shown by dotted line in figure 1.iii. All width and diameter dimensions were measured using the phase contrast images.

Seeding density	0.25 X 10^5	0.5 X 10^5	1.0 X 10^5	2.0 X 10^5	4.0 X 10^5
Average (N=3)	42.3	85.6	175.0	295.9	462.5
SD	20.7	26.2	31.9	37.4	24.9

Supplementary table 3: Number of cells in device with varying seeding density.